Independent regulation of P53 stabilisation and activation after Rb deletion in primary epithelial cells

LOUISE TREANOR, CHRISTOPHER BELLAMY, DAVID J. HARRISON and SANDRINE PROST

Division of Pathology, Queen's Medical Research Institute, 49 Little France Crescent, Edinburgh, EH16 4TJ Scotland, UK

Received January 21, 2010; Accepted March 16, 2010

DOI: 10.3892/ijo_00000650

Abstract. We have previously reported that deletion of the retinoblastoma gene *Rb* leads to rapid but transient p53 stabilisation. We investigated here the pathways involved. We show that upon Rb-deletion dysregulated E2F activates $p19^{ARF}$ expression that localises in the nucleoli. There it interacts with MDM2, leading to P53 stabilisation. At the same time, ATR is activated, activating CHK1 that may phosphorylate P53 but also contribute to inhibition of MnSOD expression leading to accumulation of ROS (reactive oxygen species) and subsequent DNA injury, which in turn maintains ATR/CHK1 activated. However, from 72 h after Rb deletion, NPM interacts with P19ARF and concomitantly the interaction between $p19^{ARF}$ and MDM2 decreases leading to a return to P53 degradation. This occurs despite the persistence of the DNA damage response pathways. We therefore observe in primary cells not subjected to exogenous gene expression or exogenous DNA damaging treatment, activation of 2 concomitant pathways of activation of P53 that are dealt with in independent manner: an oncogenic pathway with rapid activation of ARF which is 'switched off' downstream of $p19^{ARF}$ activation after 72 h of induction and a DNA damage response pathway keeping a low level of transcriptionally active P53 sufficient to deal with a physiological elevation of oxidative DNA injury. A possible connection between the two pathways is discussed.

Introduction

The retinoblastoma protein pRb is a critical regulator of cellular proliferation. It forms a complex with E2F transcription factors and inhibits their transcriptional activity. Upon phosphorylation by cyclin D-cdk4/6 in early G1 and cyclin E-cdk2 in late G1, pRb dissociates from the complex allowing E2F to activate expression of genes required for S phase. pRb is a tumor suppressor, and decreased expression is common in cancer.

Correspondence to: Dr Louise Treanor, *Present address:* Department of Hematology, St. Jude Children's Research Hospital, Memphis, TN 38105 , USA
E-mail: louise.treanor@stjude.org

Key words: ARF, Rb, cre/lox, oxidative injury, hepatocytes

Using a Cre/Lox system to specifically delete the *Rb* gene from adult mouse hepatocytes by infection with an adenovirus expressing the Cre recombinase (1,2), we are studying the early effects of the loss of *Rb*. We have previously shown *in vitro* that *Rb* deletion from primary liver cells quickly leads to dysregulated proliferation, with the concomitant appearance of multinucleated cells, cells with nuclei of abnormal morphology or cells showing abnormal mitosis reminiscent of abnormalities observed after γ-irradiation (1). Interestingly, we have also reported that in response to *Rb* deletion, P53 is rapidly stabilised and activated (2). However, this stabilisation is only transient and resolves within 4 days in culture.

P53 regulates signalling pathways controlling cell proliferation, apoptosis and DNA repair. Cellular P53 levels are normally low due to rapid degradation by the proteosome, promoted by the ubiquitin ligase and P53 partner MDM2. In response to various stimuli, the interaction of P53 with MDM2 is reduced through mechanisms ranging from post-translational modification of either protein to protein/protein interaction preventing the formation of MDM2/P53 complex (reviewed in ref. 3), thus leading to P53 stabilisation and accumulation.

In response to DNA injury, for example, various pathways are activated depending on the nature of the DNA damage and the cell type. However, all activate specific kinases that are responsible for the phosphorylation of P53 at key residues including Ser18 (Ser15 in human) (reviewed in refs. 3-6). This phosphorylation is thought to disrupt the interaction with MDM2, contribute to nuclear retention and to activate P53. The same kinases also phosphorylate other target proteins important for the regulation of cellular responses to DNA damage, which can be used as markers of DNA injury. One such marker is H2Ax, a Histone2A variant that rapidly undergoes phosphorylation on Ser139 (γH2Ax) in response to DNA damage, particularly double strand breaks (7-9).

P53 can also be stabilised in response to aberrant activation of oncogenes (10), including E2F1, in which case instability arises from activation of the ARF pathway (p14ARF in human, $p19^{ARF}$ in mouse). ARF is a nucleolar protein which can sequester MDM2 (11-13), preventing its association with P53 and restricting its E3 ligase activity (14,15). In this instance P53 is stabilised without requiring phosphorylation.

One of the critical effects of Rb deletion is to increase E2F activity (2,16). It has been reported that overexpression

of E2F activates p19ARF (17). With this in mind, we asked what pathway(s) activated after Rb deletion from otherwise genetically normal primary epithelial cells might account for the rapid but transient stabilisation of P53.

Materials and methods

Hepatocyte isolation, culture and adenovirus infection. Mouse primary hepatocytes (male, 6-12 weeks old), were isolated by a two-step retrograde liver perfusion (18) of *Rb-floxed* mice (19) and plated onto fibronectin-coated plastic in serum-free medium supplemented as previously described (1).

Wild-type and $Rb^{-/-}$ isogenic hepatocytes were obtained by infection of the hepatocytes *in vitro* with an adenovirus expressing Cre-recombinase under the human CMV promoter (Ad-Cre) or an adenovirus control (Ad-Dl70) (Virapur, USA) a multiplicity of infection of 10 (2,20). Both adenoviruses are replication-deficient (E1 deleted) serotype 5. Infection with the adenovirus expressing Cre-recombinase leads to deletion of the *Rb* gene within 16-24 h while cells infected by the adenovirus control are phenotypically wild-type.

Immunoblotting. Proteins were prepared from snap-frozen cell pellets using the appropriate lysis buffer. H2A.X, 10 mM HEPES pH 7.9, 1.5 mM $MgCl_2$, 10 mM KCl. All other proteins, 50 mM HEPES pH 7.5, 150 mM NaCl, 1 mM EDTA, 2.5 mM EGTA, 0.1% Tween-20.

Proteins were separated on SDS-PAGE and detected with a rabbit polyclonal to $p19^{ARF}$ (Ab-80 Abcam, UK), ATR (Ab10312 Abcam), ß-actin (Ab8227, Abcam), p53 (CM5, kind gift from Professor T. Hupp) phospho-p53 (9284, Cell Signalling, UK), P21 (M7202, Dako, UK) Chk1 (2345 Cell Signalling), phospho-Chk1 (2344 Cell Signalling), Chk2 (2662, Cell Signalling), NPM (15440, Abcam), mouse monoclonal to H2A.X (JBW301 Upstate, UK), MDM2 (clones 2A10 and 4B11 Calbiochem UK), sheep polyclonal to MnSOD (574596 Calbiochem), diluted in 5% Marvel TBST or TBST alone for $p19^{ARF}$ and the appropriate secondary antibodies. Proteins were visualized by ECL-plus using a versadoc4000 (Bio-Rad) to capture images and Versadoc Imaging for densitometric analysis.

Immunoprecipitation. Immunoprecipitation was performed from 400 μg of protein using TrueBlot™ (eBioscience) according to the manufacturer's instructions. Negative controls were protein A incubated with the cell lysate without antibodies.

Immunofluorescence. Hepatocytes were fixed in acetone/methanol (1:1 v/v). Immunodetection was performed using anti-P21 (mouse monoclonal M7202, Dako), anti-nucleolin (rabbit polyclonal Ab16940, Abcam) (1:100), anti-ATR (Ab10312 Abcam), mouse monoclonal anti-H2A.X (1:100) (05-636 Upstate), mouse monoclonal anti-p53 (clone pAb421, Calbiochem), anti-MDM2 (clone 2A10, Calbiochem) and rabbit polyclonal anti-$p19^{ARF}$ (1/20) (Ab-80, Abcam) and the appropriate AlexaFluor secondary antibodies (Molecular Probes, UK) followed by Topro-3 nuclear counterstain. Detection of $P19^{ARF}$ required an avidin-biotin amplification step (Sigma, UK). Where appropriate, quantification was performed by manual counting on 25 representative fields (x40) photographed with a Zeiss confocal microscope (LM510). Scanning was performed using multitracking, and settings constant throughout the experiments. Colocalisation studies were performed using Bitplane Sofware on confocal images taken with Nyquist oversampling, deconvoluted (21) using Huygens Pro 5 software (Scientific Volume Imaging).

RT-PCR. Total RNA was extracted using Qiagen RNeasy mini-column (Cat. no. 74104). cDNA was synthesised using standard protocol with MMLV (Qiagen) reverse transcriptase and an Oligo-dT primer. For real-time RT-PCR, we used Applied Biosystems 'assay by design' for E2F1 (Mm00432939_m1), GapdH (Mm99999915_q1) and custom made for p19 ARF with the following primers and probe: forward GGGCCGCACCGGAAT; reverse AAGAGCTGCT ACGTGAACGT; FAM probe CCTGGACCAGGTGATGAT. The reactions were run on an ABI PRISM 7900 Sequence Detection System (AME Bioscience).

For conventional RT-PCR, we used the following primers and annealing temperatures: ARF: forward AGGGATCCTT GGTCACTGTGAGGATTC, reverse GCAAAGCTTGAGG CCGGATTTAGCTCTGCTC at 65˚C; ß-actin forward TTCT TTGCAGCTCCTTCGTTGCCG, reverse TGGATGGCTGC GTACATGGCTGGG at 60˚C.

ROS and DNA damage quantification

8-oxo-dG. DNA was extracted using sodium iodide method (40) according to the manufacturer's recommendation (DNA Extractor WB-Kit, Wako Pure Chemical Industries, Japan). Briefly cells were lysed in a non-ionic surfactant, polyoxyethylene oxyphenyl ether buffer and spun at 10,000 g for 20 sec at 4˚C. The pellet was suspended in a SDS containing protease solution for 1 h at 37˚C. After addition of NAI the DNA was precipitated by addition of 0.5 ml of isopropyl alcohol and resuspended in water. The levels of 8-oxo-dG were measured using an ELISA kit according to the manufacturer's instructions (JaICA, Japan) in control and $Rb^{-/-}$ DNA or 8-oxo-dG standards.

AP site. Apurinic and apyrimindinic sites (AP sites) in hepatocyte DNA were detected using a DNA damage quantification kit according to the manufacturer's recommendation (K253-25 Biovision, UK). Briefly, the extracted DNA is incubated with a probe reacting with the aldehyde groups in the AP sites in the DNA, leading to the tagging with biotin residues which are detected with a colorimetric assay.

Reactive oxygen species (ROS). Measurement of ROS was done using 5-(&6)-chloromethyl-2',7'-dichlorodihydrofluorescein diacetate (CM-H2DCFDA). CM-H2DCFDA is a diacetate ester that enters passively into cells where it is cleaved by intracellular esterases leading to its retention in the cells. Reaction with intracellular ROS (hydrogen peroxide, hydroxyl radical, peroxyl radical and peroxynitrite anion) leads to emission of green fluorescence. The cells were treated with 10 μM CM-H2DCFDA and fluorescence quantified over one hour using a fluorimeter (Fluoroskan, Thermo Life Sciences) at 485 nm and 510 nm with readings taken every 3 min. This was normalised according to the amount of protein in each sample.

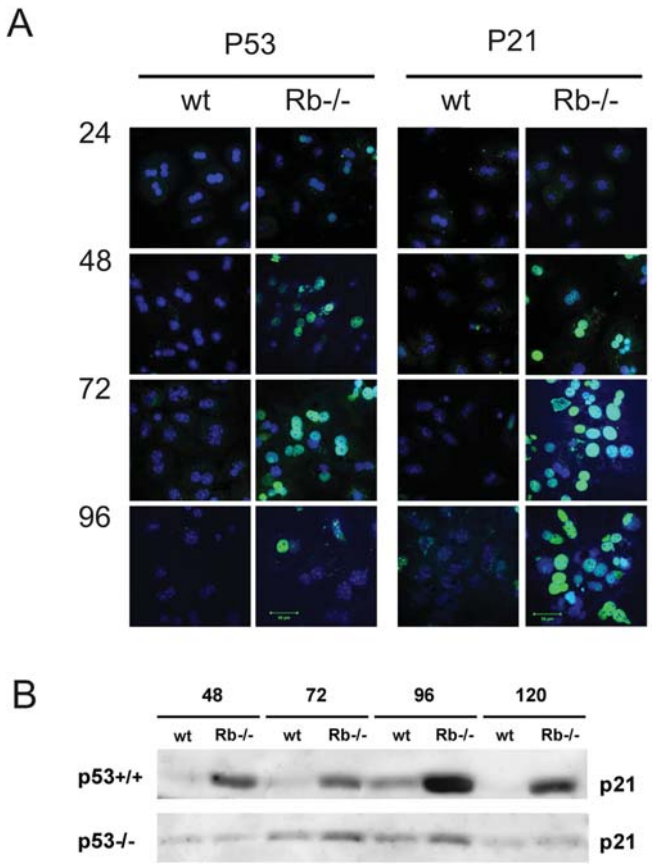

Figure 1. P53 stabilisation is transient while P21 expression remains high. (A) Immunofluorescence for P53 and P21 at indicated times after plating in $Rb^{-/-}$ and wild-type hepatocytes. Ninety-six hours after plating the number of P53 positive hepatocytes in $Rb^{-/-}$ decreases while >90% of the cells remains P21 positive. (B) p21 expression is P53-dependent. Western blotting for p21 at indicated times after plating in $Rb^{-/-}$ and wild-type hepatocytes, either wild-type or $p53^{-/-}$. In $Rb^{-/-}$ P21 is activated in a p53-dependent manner (50). The level of P21 remains high 96 and 120 h after plating, times at which P53 is no longer stabilised.

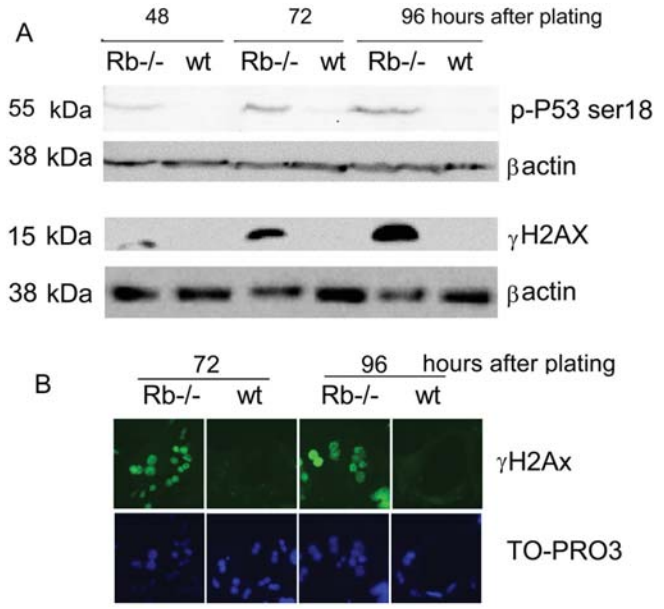

Figure 2. DNA damage markers are activated in $Rb^{-/-}$ hepatocytes. (A) Western blotting for Ser18 phosphorylation of P53 and H2AX in $Rb^{-/-}$ and control (wt) cells at indicated times after plating. ß-actin is shown as loading control. The experiment was repeated with consistent results. (B) γH2AX immunofluorescence. Photos show γH2AX immunofluorescence (green) 72 and 96 h after plating in $Rb^{-/-}$ and control (wt). TO-PRO3 is a nuclear counterstain shown here in blue.

Superoxide anion. Dihydroethidium (DHE) was used to measure the amount of superoxide anion in the hepatocytes. Upon reaction with ROS DHE is oxidised to ethidium that intercalates into the DNA and fluorescence red. Cells were incubated with DEH for 4 h, at 37˚C. Red fluorescence (567 nm) was quantified as above.

Statistical analyses. Statistical analyses were performed using Minitab 13.1 software. Effects of time and genotypes were evaluated by univariate analysis of variance (ANOVA). Differences were taken to be significant when $p<0.05$. Satisfactory homogeneity of variances was determined with Bartlett's test. Where a significant difference between means was identified, we performed pairwise comparison of means to the control using a Bonferroni correction for multiple comparisons.

Results

We have previously shown that after Rb deletion p53 is rapidly stabilised and that P21 expression is induced in a p53-dependent manner (2): 72 h after infection of primary RB-floxed hepatocytes with an adenovirus expressing the Cre recombinase, 70-80% of the cells show strong p53 and p21 nuclear positivity (2) (Fig. 1).

However, we also observed that the nuclear p53 stabilisation is only transient with the proportion of cells showing nuclear positivity decreasing sharply 80-96 h after infection (Fig. 1A). In contrast, P21 remains high and this activation is P53-dependent (Fig. 1B).

After Rb deletion, a DNA damage pathway is activated. A hallmark of P53 activation by DNA damage is phosphorylation of Ser18 (Ser15 in human). This phosphorylation was detected in $Rb^{-/-}$ cells only from 48 h after Rb deletion (Fig. 2). Further evidence to support activation of DNA damage pathways was the detection of increasing levels of γH2AX (phosphorylated at Ser139), a recognised marker of DNA damage, in $Rb^{-/-}$ cells: 96 h after Rb deletion 98-99% of $Rb^{-/-}$ cells were positive for γH2AX (Fig. 2). Both P53 and γH2AX are components of two DNA damage pathways that are driven by the DNA damage kinases ATR and ATM via checkpoint kinases 1 and 2 (Chk1 and Chk2) respectively. However, neither changes in ATM expression, nor phosphorylation of Chk2 on thr68 (target site for ATM) were detected (data not shown), suggesting that the ATM pathway is not involved here. By contrast, from 72 h after plating, ATR was found to localise in the nucleoli of 50-80% of $Rb^{-/-}$ hepatocytes (Fig. 3), suggesting activation of the protein (22). Phosphorylation of Chk1 kinase on Ser317, a site targeted by ATR was also detected in $Rb^{-/-}$ cells from 72 h, and could be inhibited by the addition of caffeine [at a concentration of 2 mM, sufficient to inhibit the activity of ATM and ATR but not DNA-PK (23)] (Fig. 3B and C). Caffeine similarly inhibited the phosphorylation of P53 at

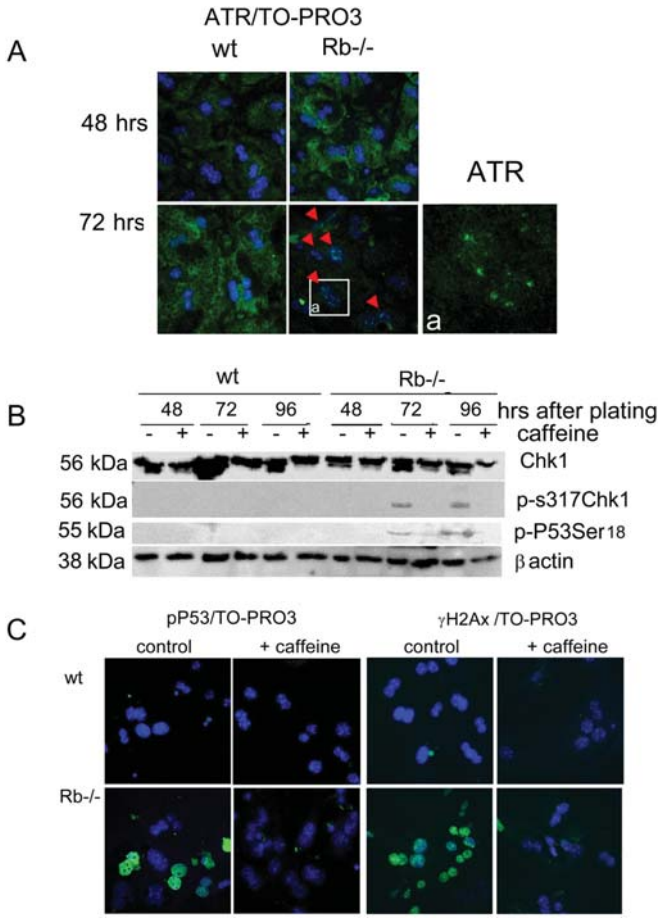

Figure 3. The ATR/Chk1 kinase pathway is activated in *Rb*$^{-/-}$ cells. (A) Immunofluorescence for ATR (green) at 48 and 72 h after plating. The blue nuclear counterstain is TO-PRO3. From 72 h after plating *Rb*$^{-/-}$ cells exhibited nucleolar staining of ATR (a). (B) Western blotting for Chk1, Ser317 phosphorylation of Chk1 and Ser18 phosphorylation of P53 in control (wt) and *Rb*$^{-/-}$ cells at indicated times after plating in the presence (+) or absence (-) of caffeine. ß-actin is shown as loading control. The experiments were repeated with consistent results. (C) Immunofluorescence for γH2AX in control (wt) and *Rb*$^{-/-}$ cells 72 h after plating in the presence (+) or absence (-) of caffeine.

Ser18 (Fig. 3B and C) and reduced γH2AX phosphorylation in *Rb*$^{-/-}$ cells (Fig. 3C).

Both E2F1 (24) and ATR activation of Chk1 kinase can inhibit NF-κB (22,25) which itself is an activator of the production of MnSOD (26) a mitochondrial enzyme catalysing superoxide anion turnover (27). We hypothetised that in *Rb*$^{-/-}$ cells the activation of E2F (2) could indirectly lead to the reduction of MnSOD expression and increased ROS leading to DNA damage and activation of the DNA damage response observed.

MnSOD protein was indeed detected 72 and 96 h after plating in control but not *Rb*$^{-/-}$ cells (Fig. 4). This is consistent with the activation of Chk1 (Fig. 3B) in *Rb*$^{-/-}$ cells indicating that there may be inhibition of MnSOD (SOD2) expression through ATR/Chk1 inhibition of the NF-κB, although this was not investigated in more detail. We then asked whether the decrease in MnSOD protein was sufficient to affect the level of endogenous ROS, with consequences for DNA damage and the observed activation of DNA damage pathways.

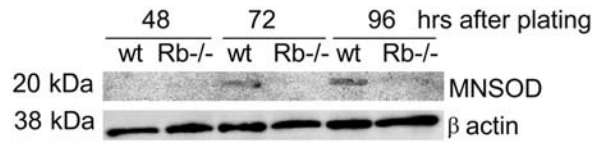

Figure 4. Inhibition of MnSOD expression in *Rb*$^{-/-}$ cells. Western blotting for MnSOD in control (wt) and *Rb*$^{-/-}$ cells at indicated times after plating.

First, we quantified ROS using two different compounds (Fig. 5A and B). From 48 h in culture ROS levels were consistently greater in *Rb*$^{-/-}$ cells compared with wild-type control (Fig. 5A) (Student's t-test p=0.03621). The same trend was observed using DHE which detected higher levels of superoxide anion in *Rb*$^{-/-}$ hepatocytes compared to wild-type controls (Fig. 5B) (asterisk denotes a significant difference using a two-tailed t-test).

We then quantified 2 types of DNA injury known to arise from ROS: 8-oxo-dG produced through the oxidation of guanine and secondly, AP sites formed via hydrolysis of the N-glycosyl bond. From 72 h in culture, the level of 8-oxo-dG rose and was greater in *Rb*$^{-/-}$ compared with control hepatocytes (Fig. 5C) (asterisk denotes a significant difference using a two-tailed t-test). This increase was also observed for AP sites, although statistical significance was not achieved (Fig. 5D, p=0.1773) which could be expected as levels of endogenously produced ROS levels are low and changes small.

Our results therefore support the hypothesis that in response to *Rb* deletion, MnSOD expression is inhibited leading to an increase in endogenous ROS with consequences for DNA damage and activation of P53. However, while the DNA damage pathway is still active 96 h after plating (H2AX activated, P53 phosphorylated on Ser18, P53-dependent activation of P21 expression, increased ROS and DNA damage); the number of hepatocytes showing P53 stabilisation decreased sharply (Figs. 1 and 6) to ~10%. This suggests that the activation of the DNA damage pathway by a low level of endogenous DNA injury, including phosphorylation of P53 on Ser18 is not sufficient to maintain high levels of P53 stabilisation. Indeed some *Rb*$^{-/-}$ hepatocytes positive for γH2AX were negative for p53 (data not shown). We investigated whether *p19*^{ARF} could be involved.

After Rb deletion, P19^{ARF} *is activated and contributes to P53 stabilisation*. E2F overexpression has been shown to induce P19ARF expression, and interaction of ARF with MDM2 stabilises P53. We therefore investigated whether P19ARF was activated in response to Rb deletion.

P19^{arf} expression was higher in *Rb*$^{-/-}$ cells compared with control (Fig. 7). It was detected from 72 h in culture by RT PCR (Fig. 7A) and from 48 h by Western blotting (Fig. 7B) in *Rb*$^{-/-}$ cells. By contrast, there was no expression detectable in control cells at early time-points and only weak expression was observed 96 h after plating. Real-time PCR confirmed an increase of ~10-fold of *p19*^{arf} expression in *Rb*$^{-/-}$ cells (Fig. 7C), and this was reduced when the cells were treated with E2F antisense (Fig. 7D).

Currently there is not one unifying model able to accurately describe the regulation of p53 by ARF in the different systems

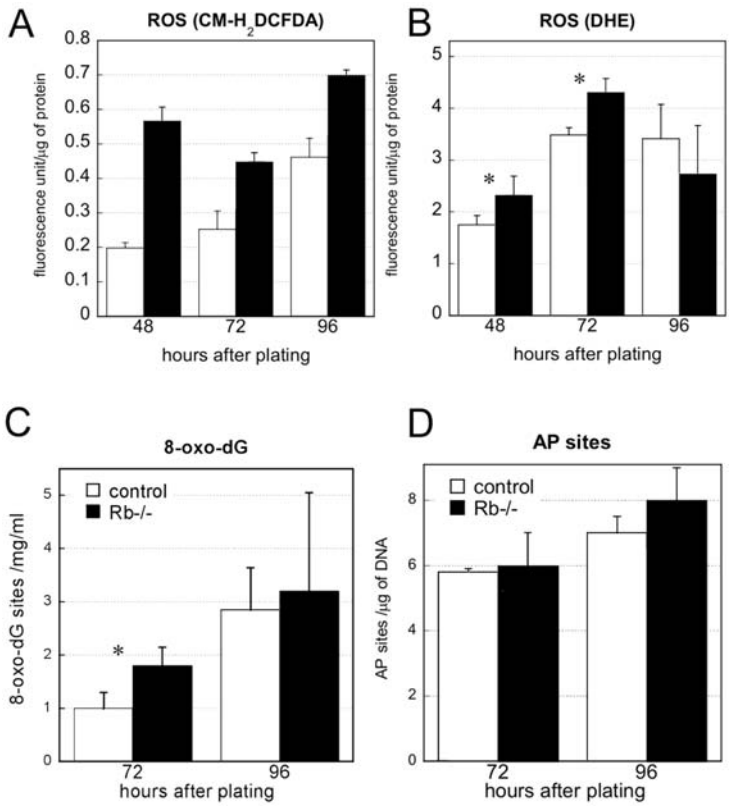

Figure 5. Reactive oxygen species (ROS) and DNA damage increase in *Rb*$^{-/-}$ cells. Quantification of the levels of ROS using CM-H_2DCFDA (A) and DHE (B). In both cases, control and *Rb*$^{-/-}$ hepatocytes (white and black bars, respectively) were incubated with the compound as described in Materials and methods. The fluorescence was quantified and normalised for the amount of protein per sample. Both assays were done in triplicate and repeated three times with consistent results. Quantification of the levels of 8-oxo-dG (C) and AP sites (D) in wt and *Rb*$^{-/-}$ hepatocytes (white and black bars, respectively). Standard curves of known concentrations of 8-oxo-dG and AP sites were used for the calculations. Both assays were performed in triplicate and repeated twice with consistent results. *Statistically significant difference (see text).

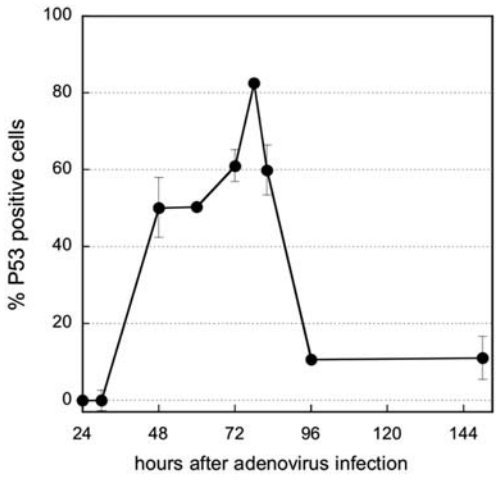

Figure 6. Quantification of P53 positive *Rb*$^{-/-}$ cells. The proportion of *Rb*$^{-/-}$ hepatocytes positive for P53 were counted at the indicated times. Five hundred cells were counted in duplicate. The values are mean ± SD.

studied. It is clear that ARF stabilises P53 through binding to MDM2, thus preventing the formation of MDM2/p53 complexes and targeting of P53 for degradation but the regulation of ARF itself seems to be different in different systems. ARF localisation and its interaction with the nucleolar protein NPM/B23 are nevertheless central to the problem and were studied next.

There were no significant differences between MDM2 protein levels detected in control and *Rb*$^{-/-}$ cells (data not shown). P19ARF immunoprecipitation pulled down MDM2 in *Rb*$^{-/-}$ cells only (Fig. 8) confirming an interaction between these proteins 48 and 72 h after plating. The interaction was greatly decreased 96 h after plating, in agreement with the decreased P53 nuclear staining observed at that time (Fig. 6). According to some models, ARF localisation is thought to affect its ability to stabilise p53. P19^{ARF} was detected in *Rb*$^{-/-}$ cells only (Fig. 9A) and localised in the nucleoli at all time-points as confirmed by co-staining with nucleolin (Fig. 9B). Quantification showed that the number of *Rb*$^{-/-}$ cells positive for P19ARF rose sharply, following the increased of P53 positive cells but remained high after 72 h when the number of P53 positive cells decreases (Fig. 9C). Thus the interaction between P19ARF with MDM2 did correlate closely with P53 stabilisation but was not regulated by a change in the localisation of P19ARF.

Nucleophosmin (NPM), a nucleolar phosphoprotein, can compete with MDM2 for interaction with P19ARF (28). We investigated if NPM was involved in the changes of interaction between MDM2 and P19ARF. Wild-type and *Rb*$^{-/-}$ hepatocytes showed similar NPM expression patterns (Fig. 10A), but immunoprecipitation with P19ARF antibodies pulled down

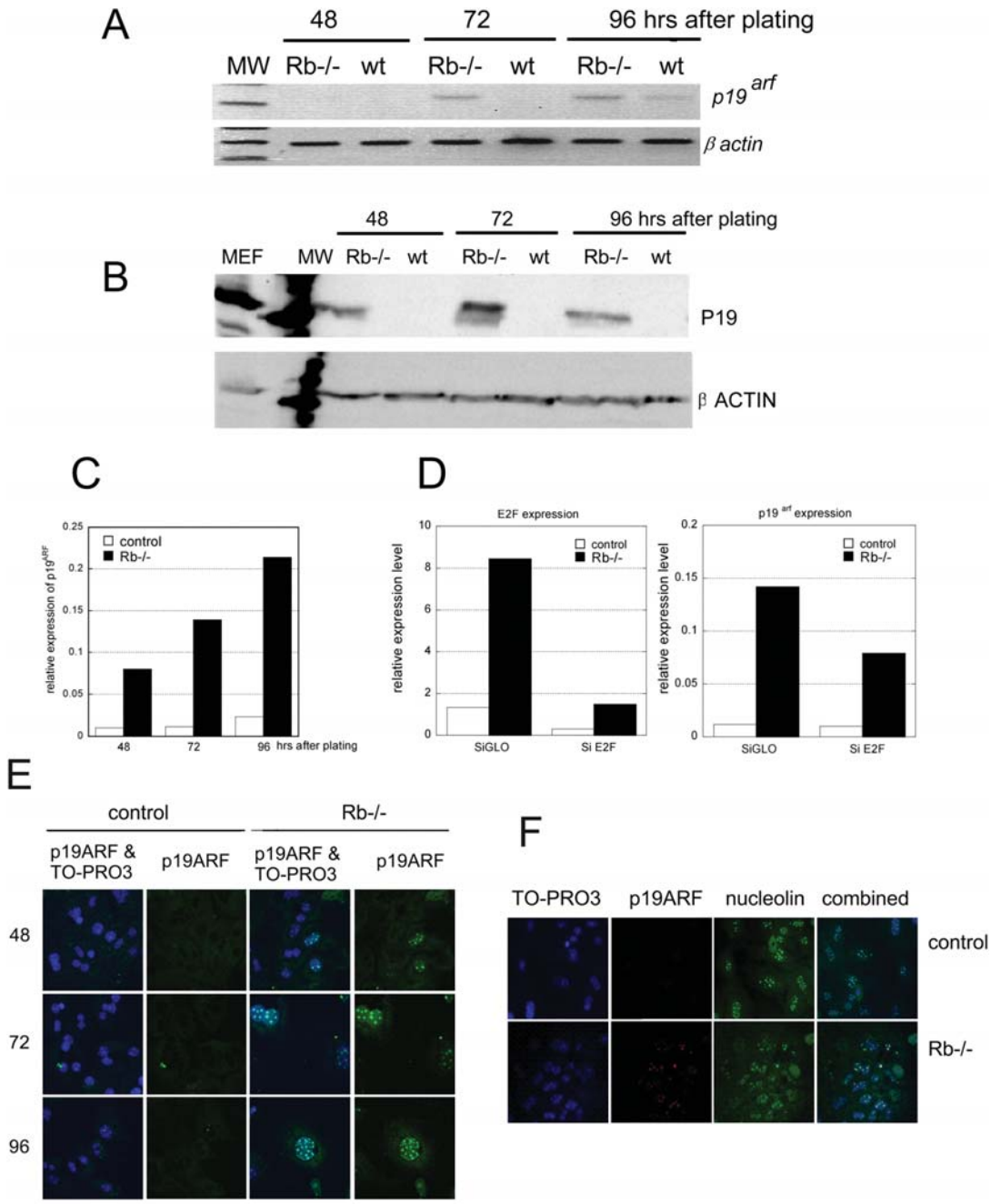

Figure 7. p19^{arf} expression is increased in *Rb*$^{-/-}$ cells and depends on increased E2F activity. (A) RTPCR for *p19arf* and *ß-actin* in control (wt) and *Rb*$^{-/-}$ cells in culture for the indicated times. (B) Western blotting for P19^{ARF} and ß-actin in control (wt) and *Rb*$^{-/-}$ cells in culture for the indicated times. (C) Real-time PCR for *p19*^{arf} expression corrected for *GAPDH* expression. (D) Real-time PCR for E2F and *p19*^{arf} expression corrected for *GAPDH* expression in control and *Rb*$^{-/-}$ cells in culture for 72 h, treated with E2F antisense for 30 h. The results for E2F expression after treatment with antisense has already been published by the authors (16). (C and D) White bars, control; black bars, *Rb*$^{-/-}$ hepatocytes.

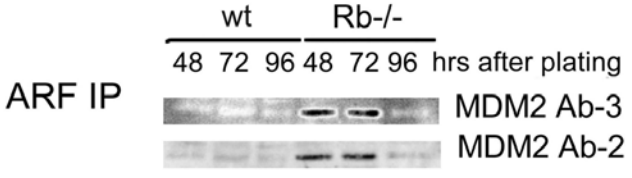

Figure 8. P19ARF interacts with MDM2 in *Rb*$^{-/-}$ cells. Proteins isolated from control (wt) and *Rb*$^{-/-}$ samples at indicated times were immunoprecipitation with an antibody to p19^{ARF}. The precipitates were immunoblotted for MDM2 using to 2 different antibodies Ab2 (2A10) and Ab3 (4B11) which recognize different regions of the protein.

NPM in *Rb*$^{-/-}$ only, showing an interaction between the two proteins from 72 h after plating (Fig. 10B).

Discussion

Oncogenic stimuli leading to P53 stabilisation are complex as they can potentially trigger multiple apparently unrelated pathways. An example is shown here using primary epithelial cells, where a physiological increase in E2F activity is obtained in response to acute *Rb* deletion. On one hand, increased E2F activity activates the expression of ARF which interacts

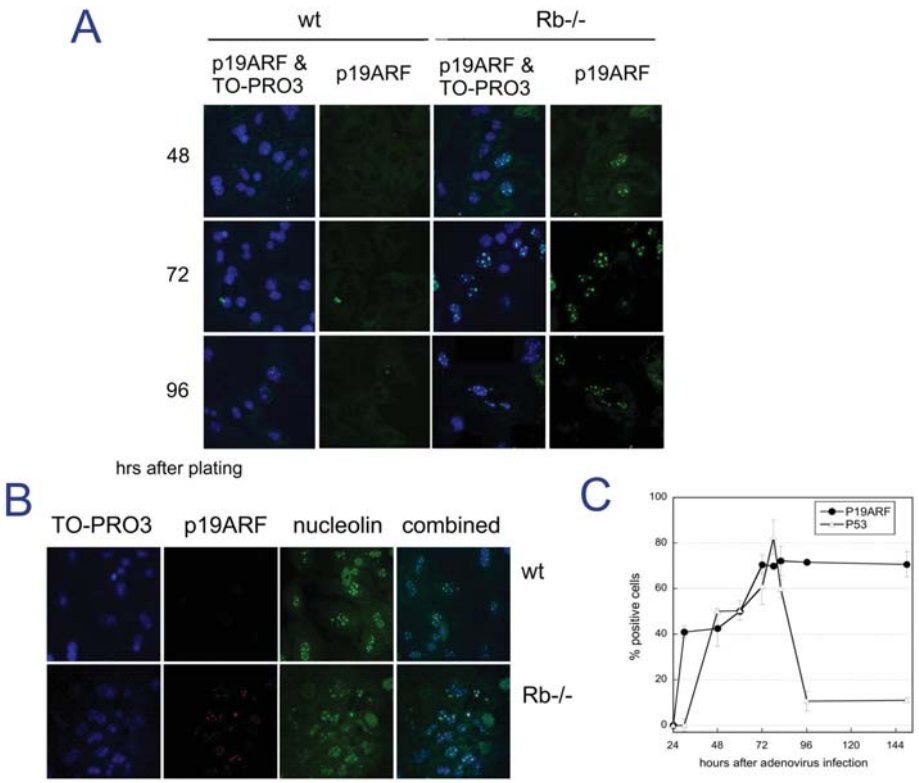

Figure 9. ARF localised in the nucleoli. (A) Immunofluorescence for P19ARF in control (wt) and *Rb*$^{-/-}$ cells 48, 72 and 96 h after plating. Green fluorescence, P19ARF; blue fluorescence, nuclear counterstain with TO-PRO3. (B) Double immunofluorescence for P19ARF and nucleolin in control (wt) and *Rb*$^{-/-}$ cells, 72 h after plating. Red fluorescence, P19ARF; green fluorescence, nucleolin; blue fluorescence, nuclear counterstain with TO-PRO3. (C) Graph showing the quantification of P53 and ARF positive *Rb*$^{-/-}$ cells at indicated time. Note that the number of cells positive for ARF remains high while the number of P53 positive cells decreases after 78 h.

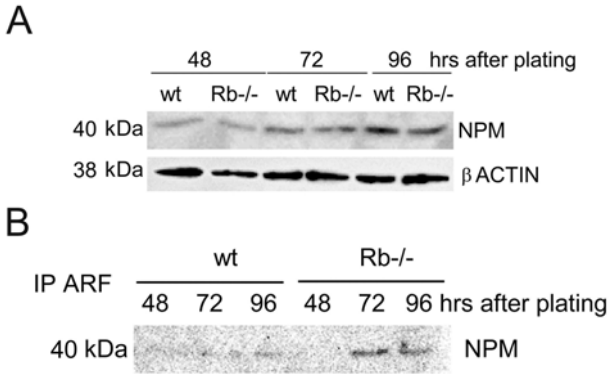

Figure 10. NPM is expressed in hepatocytes and interacts with P19ARF in *Rb*$^{-/-}$ cells 96 h after plating. (A) NPM expression in control (wt) and *Rb*$^{-/-}$ hepatocytes at indicated times after plating. (B) Immunoprecipitation with P19ARF antibodies. Control (wt) and *Rb*$^{-/-}$ proteins were immunoprecipitated with an antibody against p19^{ARF} and probed with an antibody against NPM at indicated times after plating.

with MDM2 and contributes to P53 stabilisation. On the other hand, E2F leads to decreased MnSOD expression, accumulation of reactive oxygen species and DNA damage, triggering a DNA injury response that can activate P53 through post-translational modifications including phosphorylation of Ser18. While the DNA damage response is sustained, the stabilisation of P53 resolves within 96 h showing that the two pathways are regulated independently.

Rb deletion leads to DNA injury. Based on our data and others we suggest the following model: upon Rb deletion, E2F activation leads to *Arf* induction, ATM/Chk1 activation which can inhibit relA (NF-κB) (22). This relA inhibition leads to decreased MnSOD (SOD2) expression resulting in accumulation of endogenous ROS leading to DNA injury and activation of DNA damage pathways: activation of ATR/chk1, γH2AX and phosphorylation of P53. Interestingly, others have also observed activation of γH2AX in response to Rb deletion (29,30). However, these studies clearly suggest that γH2AX is not associated with ROS induced DNA damage (30) but rather with DSB induced at the replication fork (29). Although in some cases activation of ATM/chk2 or ATR/chk1 are clearly associated with a specific type of DNA injury, often the situation is more complex with simultaneous activation and/or interconnection of the two pathways. Pickering and Kowalik found that γH2AX induction in response to *Rb* deletion was ATM-independent supporting our result (30). By contrast in response to TWIST depletion, which activates ARF, γH2AX increases together with activation of both chk1 and chk2 kinases (31). This suggests that activation of γH2AX in response to *Rb* deletion and/or ARF over-expression may result from a combination of DNA damage pathways that may be cell type specific. In summary, the increased ROS and γH2AX activation clearly shows that *Rb* loss leads to DNA injury and P53 stabilisation. In fact this could be contributing to the early activation of DNA damage checkpoints observed in early human carcinogenesis (32).

Arf-dependent regulation of P53 stabilisation. Interestingly, we observed a dynamic regulation of P53 with rapid but transient stabilisation, then return to low protein levels, which was correlated with ARF-MDM2 interaction. The currently favoured model of regulation of P53 by ARF suggests that in the nucleoli, ARF is sequestered by NPM and unable to interact with MDM2. In that model, in response to high levels of DNA injury, ARF relocalises to the nucleoplasm where it binds to MDM2, leading to P53 stabilisation (reviewed in refs. 33,34).

In the present system, where gene expressions are endogenous, we confirm that ARF interaction with MDM2 dictates the level of P53 protein and that interaction between ARF and MDM2 is abolished by NPM binding to ARF. However this change in interaction occurs without dissociation of the nucleoli or relocalisation of ARF. Brady *et al* (28) have recently demonstrated that ARF/NPM and ARF/MDM2 are independent protein complexes. Interestingly, they also demonstrated a binding preference of ARF for MDM2 over NPM suggesting that an active regulation must take place for the binding to change from MDM2 to NPM. NPM has been shown to be induced by exogenous DNA damage (35,36) and a difference in the stoichiometry between MDM2 and NPM could be sufficient to affect the binding partner (28,34), even in absence of damage to the nucleoli structure. However, we did not observe a change in NPM protein level suggesting that another mechanism is involved for the observed regulation of ARF binding to MDM2. We have observed in $Rb^{-/-}$ cells homodimeric forms of P19ARF at the time of decreased interaction with MDM2 (data not shown). ROS have been shown to induce homodimerisation of the human form of P19ARF (P14ARF) which leads to a decreased affinity for HDM2 (37). Based on this work in human cells and our own work, we postulate that in response to *Rb* deletion, increased endogenous ROS may promote homodimerisation of P19ARF at late time-points leading to a decrease affinity for MDM2. NPM can bind to ARF leading to a return to MDM2-dependent degradation of P53.

Feed-back loops and interaction of two pathways. P53 is critical in the regulation of many cellular responses and (the) many ways by which P53 activity can be regulated are now clearly established. However, as discussed by Harris and Levine, the regulatory mechanisms have often been studied in established, frequently transformed cell lines, which are likely to bear various mutations, using overexpression vectors, mutant proteins and/or high levels of DNA damage (38). The many feed-back loops that exist are likely to provide a different picture in a physiological system.

Using primary epithelial cells, in which *Rb* is deleted acutely, we have shown how deletion of *Rb* can trigger 2 pathways of activation of P53 which may be interconnected but are regulated independently: P53 remains transcriptionally active at times when NPM interacts with ARF and the overall P53 protein level has returned to baseline. This suggests that P53 stabilisation and activation are independent in this setting as previously suggested by others (39). ARF has been reported to promote some post-translational modifications liable to activate P53 such as acetylation (40,41) or ATM dependent phosphorylation on Ser15 (42), however, these modifications can also be activated by DNA damage pathways whose activation was not ruled out in those studies. By contrast P53 can be stabilised without phosphorylation on Ser15 (43) supporting our hypothesis that *arf* overexpression stabilises P53 but activation itself results from another pathway, activation of ATR/Chk1pathway by ROS-induced DNA damage.

This regulation may provide a mechanism where the cells are able to sense the level of stress and prevent P53 stabilisation, possibly until the stress is such that elimination of the cells is necessary (44). The role of P53 in controlling apoptosis needs indeed to be tightly controlled to allow its activity in regulating other critical cellular pathways such as proliferation and differentiation.

This is supported by work suggesting that interaction between NPM and ARF has a regulatory role by promoting the accumulation of inactive ARF until it is required, and thus could set a threshold for P53 response (45,46). In the presence of high level of DNA injury, such as in studies involving UV-induced DNA damage (47) NPM can repress P53 activation until the levels of damage are such that DNA repair pathways or apoptosis should be activated (46,47). In this case the high level of DNA damage promotes a redistribution of ARF; NPM/ARF complexes disappear from the nucleoli and ARF complexes with MDM2 in the nuclei (47) although this may be due to damage to the nucleoli itself rather than to the DNA (48). A recent study further suggests that redistribution of ARF may be limited to DNA damage that induces the JNK pathway (49). In the absence of JNK induction, as observed after ionising radiation (49), ARF could be activated without relocalisation as observed in the present study.

In conclusion, the present data from primary cells suggests that the mdm2/p53/NPM/ARF pathway provides a pathophysiologic sensor mechanism allowing inhibition of proliferation by low levels of active P53, perhaps giving the opportunity for DNA repair to occur, while apoptosis is inhibited. In normal cells, a low level of ROS and DNA damage activates sufficient P53 to induce P21 and lead to cell cycle arrest. However, the overall amount of P53 protein would be kept low as NPM interacts with ARF and P53 is targeted to degradation by MDM2. Additional signal, such as high levels of damage could activate ARF and stabilisation of P53 would allow induction of apoptosis. This mechanism allows to maintain P53 below the threshold necessary for cell death (44).

Acknowledgments

We thank Helen Caldwell for technical assistance. The Rb-floxed ($Rb^{lox/lox}$) mice were a kind gift from Anton Berns (Netherlands Cancer Institute, Amsterdam) to whom we are very grateful. The University of Edinburgh is a charitable body, registered in Scotland, with registration number SC005336. This work was supported by grants from the Melville Trust for the Care and Cure of Cancer to S.P. The experiment for Fig. 1B was performed by Sharon Sheahan, who we gratefully acknowledge.

References

1. Sheahan S, Bellamy C, Dunbar D, Harrison D and Prost S: Deficiency of G1 regulators P53, P21CIP and/or pRb decreases hepatocyte sensitivity to TGFß cell cycle arrest. BMC Cancer 7: 215-255, 2007.

2. Sheahan S, Bellamy COC, Treanor L, Harrison DJ and Prost S: Additive effect of p53, p21 and Rb deletion in triple knockout primary hepatocytes. Oncogene 23: 1489-1497, 2004.
3. Xu Y: Regulation of p53 responses by post-translational modifications. Cell Death Differ 10: 400-403, 2003.
4. Sancar A, Lindsey-Boltz LA, Unsal-Kacmaz K and Linn S: Molecular mechanisms of mammalian DNA repair and the DNA damage checkpoints. Annu Rev Biochem 73: 39-85, 2004.
5. Helton ES and Chen X: p53 modulation of the DNA damage response. J Cell Biochem 100: 883-896, 2007.
6. Chen YW, Klimstra DS, Mongeau ME, Tatem JL, Boyartchuk V and Lewis BC: Loss of p53 and Ink4a/Arf cooperate in a cell autonomous fashion to induce metastasis of hepatocellular carcinoma cells. Cancer Res 67: 7589-7596, 2007.
7. Tanaka T, Halicka HD, Huang X, Traganos F and Darzynkiewicz Z: Constitutive histone H2AX phosphorylation and ATM activation, the reporters of DNA damage by endogenous oxidants. Cell Cycle 5: 1940-1945, 2006.
8. Foster ER and Downs JA: Histone H2A phosphorylation in DNA double-strand break repair. FEBS J 272: 3231-3240, 2005.
9. Escargueil AE, Soares DG, Salvador M, Larsen AK and Henriques JA: What histone code for DNA repair? Mutat Res 658: 259-270, 2008.
10. Vousden KH: p53: Death star. Cell 103: 691-694, 2000.
11. Weber JD, Taylor LJ, Roussel MF, Sherr CJ and Bar-Sagi D: Nucleolar Arf sequesters Mdm2 and activates p53. Nat Cell Biol 1: 20-26, 1999.
12. Tao W and Levine AJ: P19(ARF) stabilizes p53 by blocking nucleo-cytoplasmic shuttling of Mdm2. Proc Natl Acad Sci USA 96: 6937-6941, 1999.
13. Sherr CJ: Divorcing ARF and p53: an unsettled case. Nat Rev Cancer 6: 663-673, 2006.
14. Honda R and Yasuda H: Association of p19(ARF) with Mdm2 inhibits ubiquitin ligase activity of Mdm2 for tumor suppressor p53. EMBO J 18: 22-27, 1999.
15. Weber JD, Kuo ML, Bothner B, Di Giammarino EL, Kriwacki RW, Roussel MF and Sherr CJ: Cooperative signals governing ARF-mdm2 interaction and nucleolar localization of the complex. Mol Cell Biol 20: 2517-2528, 2000.
16. Prost S, Lu P, Caldwell H and Harrison D: E2F regulates DDB2: consequences for DNA repair in Rb-deficient cells. Oncogene 26: 3572-3581, 2007.
17. Bates S, Phillips AC, Clark PA, Stott F, Peters G, Ludwig RL and Vousden KH: $p14^{ARF}$ links the tumour suppressors RB and p53. Nature 395: 124-125, 1998.
18. Bellamy CO, Clarke AR, Wyllie AH and Harrison DJ: p53 deficiency in liver reduces local control of survival and proliferation, but does not affect apoptosis after DNA damage. FASEB J 11: 591-599, 1997.
19. Vooijs M, Riele HT, van der Valk M and Berns A: Tumor formation in mice with somatic inactivation of the retinoblastoma gene in interphotoreceptor retinol binding protein-expressing cells. Oncogene 21: 4635-4645, 2002.
20. Prost S, Sheahan S, Rannie D and Harrison DJ: Adenovirus-mediated Cre deletion of floxed sequences in primary mouse cells is an efficient alternative for studies of gene deletion. Nucleic Acids Res 29: art-e80, 2001.
21. Landmann L: Deconvolution improves colocalization analysis of multiple fluorochromes in 3D confocal data sets more than filtering techniques. J Micros Oxford 208: 134-147, 2002.
22. Rocha S, Garrett MD, Campbell KJ, Schumm K and Perkins ND: Regulation of NF-kappaB and p53 through activation of ATR and Chk1 by the ARF tumour suppressor. EMBO J 24: 1157-1169, 2005.
23. Sarkaria JN, Busby EC, Tibbetts RS, Roos P, Taya Y, Karnitz LM and Abraham RT: Inhibition of ATM and ATR kinase activities by the radiosensitizing agent, caffeine. Cancer Res 59: 4375-4382, 1999.
24. Tanaka H, Matsumura I, Ezoe S, *et al*: E2F1 and c-Myc potentiate apoptosis through inhibition of NF-kappaB activity that facilitates MnSOD-mediated ROS elimination. Mol Cell 9: 1017-1029, 2002.
25. Rocha S and Perkins ND: ARF the integrator: linking NF-kappaB, p53 and checkpoint kinases. Cell Cycle 4: 756-759, 2005.
26. Jones PL, Ping DS and Boss JM: Tumor necrosis factor alpha and interleukin-1 beta regulate the murine manganese superoxide dismutase gene through a complex intronic enhancer involving C/EBP-beta and NF-kappa B. Mol Cell Biol 17: 6970-6981, 1997.
27. Oberley LW: Mechanism of the tumor suppressive effect of MnSOD overexpression. Biom Pharm 59: 143-148, 2005.
28. Brady SN, Yu Y, Maggi LB and Weber JD: ARF impedes NPM/B23 shuttling in an Mdm2-sensitive tumor suppressor pathway. Mol Cell Biol 24: 9327-9338, 2004.
29. Bosco EE, Mayhew CN, Hennigan RF, Sage J, Jacks T and Knudsen ES: RB signaling prevents replication-dependent DNA double-strand breaks following genotoxic insult. Nucleic Acids Res 32: 25-34, 2004.
30. Pickering MT and Kowalik TF: Rb inactivation leads to E2F1-mediated DNA double-strand break accumulation. Oncogene 25: 746-755, 2006.
31. Kwok WK, Ling MT, Yuen HF, Wong YC and Wang X: Role of $p14^{ARF}$ in TWIST-mediated senescence in prostate epithelial cells. Carcinogenesis 28: 2467-2475, 2007.
32. Bartkova J, Horejsi Z, Koed K, *et al*: DNA damage response as a candidate anti-cancer barrier in early human tumorigenesis. Nature 434: 864-870, 2005.
33. Zhang Y and Xiong Y: A p53 amino-terminal nuclear export signal inhibited by DNA damage-induced phosphorylation. Science 292: 1910-1915, 2001.
34. Gjerset RA and Bandyopadhyay K: Regulation of $p14^{ARF}$ through subnuclear compartmentalization. Cell Cycle 5: 686-690, 2006.
35. Khan SH, Moritsugu J and Wahl GM: Differential requirement for $p19^{ARF}$ in the p53-dependent arrest induced by DNA damage, microtubule disruption, and ribonucleotide depletion. Proc Natl Acad Sci USA 97: 3266-3271, 2000.
36. Khan S, Guevara C, Fujii G and Parry D: $p14^{ARF}$ is a component of the p53 response following ionizing irradiation of normal human fibroblasts. Oncogene 23: 6040-6046, 2004.
37. Menendez S, Khan Z, Coomber DW, Lane DP, Higgins M, Koufali MM and Lain S: Oligomerization of the human ARF tumor suppressor and its response to oxidative stress. J Biol Chem 278: 18720-18729, 2003.
38. Harris SL and Levine AJ: The p53 pathway: positive and negative feedback loops. Oncogene 24: 2899-2908, 2005.
39. Toledo F and Wahl GM: Regulating the p53 pathway: *in vitro* hypotheses, *in vivo* veritas. Nat Rev Cancer 6: 909-923, 2006.
40. Ito A, Lai CH, Zhao X, Saito S, Hamilton MH, Appella E and Yao TP: p300/CBP-mediated p53 acetylation is commonly induced by p53-activating agents and inhibited by MDM2. EMBO J 20: 1331-1340, 2001.
41. Mellert H, Sykes SM, Murphy ME and McMahon SB: The ARF/oncogene pathway activates p53 acetylation within the DNA binding domain. Cell Cycle 6: 1304-1306, 2007.
42. Li J, Zhang XL, Sejas DP, Bagby GC and Pang QS: Hypoxia-induced nucleophosmin protects cell death through inhibition of p53. J Biol Chem 279: 41275-41279, 2004.
43. De Stanchina E, McCurrach ME, Zindy F, *et al*: E1A signaling to p53 involves the p19(ARF) tumor suppressor. Genes Dev 12: 2434-2442, 1998.
44. Nakano H, Yonekawa H and Shinohara K: Threshold level of p53 required for the induction of apoptosis in X-irradiated MOLT-4 cells. Int J Radiat Oncol Biol Phys 68: 883-891, 2007.
45. Korgaonkar C, Hagen J, Tompkins V, Frazier AA, Allamargot C, Quelle FW and Quelle DE: Nucleophosmin (B23) targets ARF to nucleoli and inhibits its function. Mol Cell Biol 25: 1258-1271, 2005.
46. Maiguel DA, Jones L, Chakravarty D, Yang C and Carrier F: Nucleophosmin sets a threshold for p53 response to UV radiation. Mol Cell Biol 24: 3703-3711, 2004.
47. Lee C, Smith BA, Bandyopadhyay K and Gjerset RA: DNA damage disrupts the p14ARF-B23 (nucleophosmin) interaction and triggers a transient subnuclear redistribution of $p14^{ARF}$. Cancer Res 65: 9834-9842, 2005.
48. Rubbi CP and Milner J: Disruption of the nucleolus mediates stabilization of p53 in response to DNA damage and other stresses. EMBO J 22: 6068-6077, 2003.
49. Yogev O, Saadon K, Anzi S, Inoue K and Shaulian E: DNA damage-dependent translocation of B23 and p19 ARF is regulated by the Jun N-terminal kinase pathway. Cancer Res 68: 1398-1406, 2008.